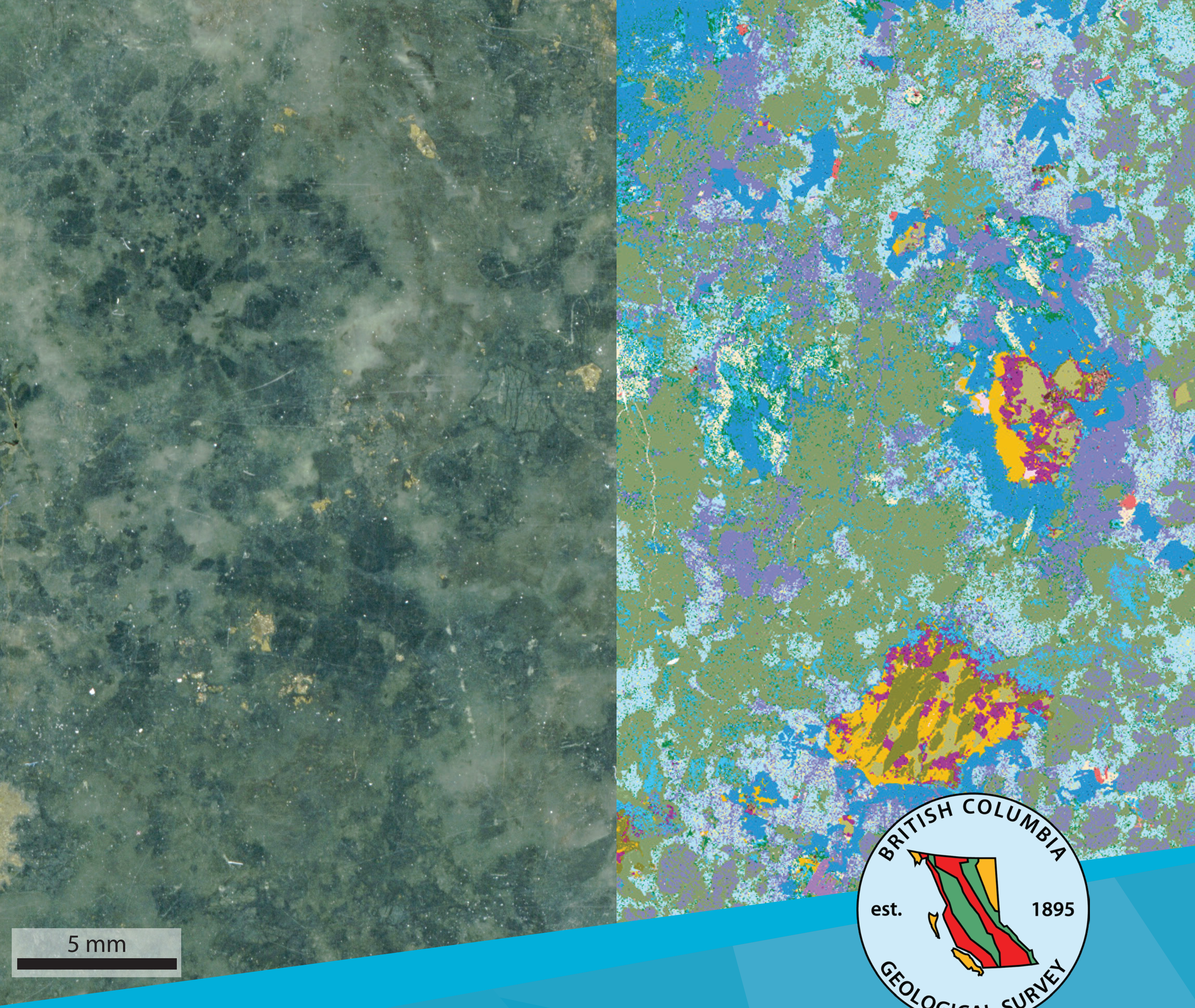

British Columbia Geological Survey
est. 1895

Data release from critical mineral study of the E&L magmatic sulphide deposit, Nickel mountain, British Columbia: Whole-rock geochemical and scanning electron microscopy-mineral liberation analysis (SEM-MLA) data

Matthew J. Brzozowski, Audrey C. Graham, Keanna Vaughan Forrester, Luke Ootes, and Dylan Goudie

British Columbia
Ministry of
Mining and
Critical Minerals

GeoFile 2026-08

Ministry of Mining and Critical Minerals
Mines Competitiveness and Authorizations Division
British Columbia Geological Survey

Recommended citation: Brzozowski, M.J., Graham, A.C., Vaughan Forrester, K., Ootes, L., and Goudie, D., 2026. Data release from critical mineral study of the E&L magmatic sulphide deposit, Nickel mountain, British Columbia: Whole-rock geochemical and scanning electron microscopy-mineral liberation analysis (SEM-MLA) data. British Columbia Ministry of Mining and Critical Minerals, British Columbia Geological Survey GeoFile 2026-08, 3 p.

Front Cover:
Coarse-grained taxitic gabbro of the E&L intrusion. Photograph of thin section billet and corresponding SEM-MLA image showing pentlandite in association with chalcopyrite-pyrite-chalcopyrite in chloritized groundmass (sample D23MBR-1-4).

Back Cover:
Mountainous terrain in region of E&L deposit.

Ministry of
Mining and
Critical Minerals

Data release from critical mineral study of the E&L magmatic sulphide deposit, Nickel mountain, British Columbia: Whole-rock geochemical and scanning electron microscopy-mineral liberation analysis (SEM-MLA) data

M.J. Brzozowski
A.C. Graham
K. Vaughan Forrester
L. Ootes
D. Goudie

Ministry of Mining and Critical Minerals
British Columbia Geological Survey

GeoFile 2026-08

Data release from critical mineral study of the E&L magmatic sulphide deposit, Nickel mountain, British Columbia: Whole-rock geochemical and scanning electron microscopy-mineral liberation analysis (SEM-MLA) data

Matthew J. Brzozowski[1], Audrey C. Graham[2, a], Keanna Vaughan Forrester[2], Luke Ootes[2], and Dylan Goudie[3]

[1] Key Laboratory of Western China's Mineral Resources and Geological Engineering, Ministry of Education, School of Earth Science and Resources, Chang'an University, Xi'an 710054, China
[2] British Columbia Geological Survey, Ministry of Mining and Critical Minerals, Victoria, BC, V8W 9N3
[3] Core Research Equipment and Instrument Training (CREAIT) Network, Memorial University of Newfoundland, St. John's, NL, A1C 5S7
[a] corresponding author: Audrey.Graham@gov.bc.ca

Recommended citation:Brzozowski, M.J., Graham, A.C., Vaughan Forrester, K., Ootes, L., and Goudie, D., 2026. Data release from critical mineral study of the E&L magmatic sulphide deposit, Nickel mountain, British Columbia: Whole-rock geochemical and scanning electron microscopy-mineral liberation analysis (SEM-MLA) data. British Columbia Ministry of Mining and Critical Minerals, British Columbia Geological Survey GeoFile 2026-08, 3 p.

Abstract

Magmatic sulphide deposits are the principal resource of platinum-group elements (PGE) and Ni globally, and significant contributors of Cu and Co. Considering that the global supplies of PGE, Ni, and Co are controlled by few countries and their importance in a number of industries, they are considered critical minerals by numerous jurisdictions worldwide. In British Columbia, the vast majority of magmatic sulphide deposits occur in Alaskan-type and other mafic-ultramafic intrusions in Quesnel and Stikine terranes. Although work has been done on the larger deposits, such as Giant Mascot, little has been done to characterize the other deposits, making it difficult to understand their petrogenesis and economic significance.

This contribution provides whole-rock geochemical data for 100 drill core and outcrop samples collected from the E&L deposit. The data comprise rocks from the E&L pluton (n=55), Nickel mountain gabbroic complex (n=29), and local Spatsizi Formation (n=10), as well as rocks from under an ice sheet on Nickel mountain to the northeast of the E&L deposit (n=6). Mineral abundance data and mineral maps of ten thin sections are also provided, which were determined by scanning electron microprobe-mineral liberation analysis (SEM-MLA).

Keywords: Magmatic sulphide deposit, base and precious metals, Ni-Cu-PGE, critical minerals

---

1. Introduction

Magmatic sulphide deposits are the principal resource of platinum-group elements (PGE) and Ni globally (Mudd and Jowitt, 2014; Mudd et al., 2018). Although Co resources are predominantly in sediment-hosted Cu-Co (~63%) and Ni-Co laterite deposits (~20%), magmatic sulphide deposits are also significant contributors (~14%; Mudd et al., 2013; Petavratzi et al., 2019). Considering that the global supplies of PGE, Ni, and Co are controlled by three countries (South Africa, Bushveld Complex; Russia, Norilsk Talnakh camp; Democratic Republic of the Congo) they are considered at risk of supply disruptions and/or shortages (Mudd et al., 2013, 2018; Mudd and Jowitt, 2014; Petavratzi et al., 2019). This, alongside their value in low-carbon technologies, and the defense, energy, aerospace, and electronics industries, has caused numerous jurisdictions worldwide to label them as critical minerals (e.g., Humphreys, 2014; Reich and Simon, 2025).

Magmatic sulphide deposits typically occur in areas where a mantle plume has impinged upon the lithosphere (Ernst and Jowitt, 2013). In British Columbia however, magmatic sulphide deposits are almost exclusively associated with rocks in Quesnel and Stikine terranes that formed in a convergent margin, including Giant Mascot (Manor et al., 2016), Turnagain (Jackson-Brown, 2017), Polaris (Milidragovic et al., 2021), and E&L (Brzozowski and Zaborniak, 2024). Many of these magmatic sulphide deposits remain poorly characterized, making it difficult to assess their petrogenesis. Herein we present data from the E&L magmatic sulphide deposit and spatially associated mafic-ultramafic and sedimentary rocks (BCGS_GF2026-08.zip). Appendix 1 provides the whole-rock geochemistry, Appendix 2 the modal mineralogy of thin sections from SEM-MLA, and Appendix 3 mineral maps of these thin sections.

2. Methods

2.1. Whole-rock geochemistry

2.1.1. Sample preparation

A total of 100 samples for geochemistry were collected from drill core (n=95) and outcrop (n=5) during August-September 2023. The samples were cut at the BCGS and sent to ALS Canada Ltd. (North Vancouver) for preparation using the PREP-31 package, which includes crushing the samples to 70% passing 2 mm, riffle splitting off 250 g of this material, and pulverizing this split to better than 85% passing 75 µm. Remaining sample material, crush, and pulp were archived.

2.1.2. Analytical methods

The geochemistry of whole-rock samples was determined at ALS Canada Ltd. using the CCP-PKG01 complete characterization package (ALS, 2024). Samples that returned greater than the detection range for specific analytes were re-analyzed with ore-grade methods while maintaining consistency in the digestion method (Appendix 1, Attributes). For analytes that yielded greater than detection ranges, results from the ore-grade methods supersede previous results.

Major-element oxides were determined using the ME-ICP06 method (ALS, 2024). A 0.1 g subsample was mixed with a Li borate flux and fused in a furnace at 1025°C. The melt was cooled and dissolved in nitric, hydrochloric, and hydrofluoric acid and the resultant solution was analyzed by inductively coupled plasma (ICP) atomic emission spectroscopy (AES). Results were corrected for inter-element spectral interference before being reported. Total (%) and loss on ignition (LOI%) values are included. Trace (lithophile) elements (e.g., Ba, Ga, Ge, Sn, U, V, W) were determined using the ME-MS81 method (ALS, 2024), which uses the same Li borate fusion and acid digestion as ME-ICP06 followed by ICP-mass spectrometry (MS) analysis. This fusion is considered the best method for complete dissolution of silicates, although some zircon, metal oxides, rare-earth phosphates, and sulphides may not be fully recovered (ALS, 2024).

Base metals (Ag, Cd, Co, Cu, Li, Mo, Ni, Pb, and Zn) were determined using the ME-4ACD81 method, which uses ICP-AES following Li borate fusion and digestion of a 0.25 g subsample in a 4-acid (perchloric, nitric, hydrofluoric, hydrochloric) solution. Samples that yielded greater than the detection ranges (100 ppm Ag, 1000 ppm Cd, or 1% of Pb, Zn, and Cu) were re-analyzed for single analytes using the ME-OG62 method, a 4-acid digestion on 0.4 g subsample followed by ICP-AES analysis.

Carbon and S were analyzed by LECO infrared spectroscopy (ME-IR08) in which a sample is combusted in a high-frequency LECO induction furnace in a stream of oxygen that converts S into SO_2 and C into CO_2. The resultant gas was passed directly into a cell with infrared (IR) energy, which absorbed the SO_2 and CO_2 at different wavelengths. Absorption was quantitatively detected and used to calculate total S and total C.

Volatile trace elements (e.g., As, Bi, Hg, In, Sb, Te) were determined using the ME-MS42 method (ALS, 2024). A 0.5 g subsample was dissolved in aqua regia for 45 minutes, diluted to 12.5 mL with de-ionized water, and analyzed by ICP-MS with collision cell. These elements were analyzed using relatively low-temperature aqua regia digestion to avoid volatilization as is common with higher temperature 4-acid digestion or fusion methods.

The platinum group metals (Pt, Pd, Rh, Ir, Os, and Ru) were analyzed by nickel sulphide collection fire assay with ICP-MS finish (PGM-MS25NS; ALS, 2024).

2.1.3. Quality assurance

A total of 10 quality control samples (silica blanks, pulp duplicates, and standards) were inserted into the sample stream at the BCGS preparatory laboratory (Appendix 1, Data).

2.1.3.1. Preparation blanks

To monitor sample preparation contamination, four coarse silica sand blanks (Sigma-Aldrich-certified as ≥99.995 wt.% SiO_2) were pulverized in the same manner as routine samples (Appendix 1, Blanks-contamination). The Cu and Ni contents of the analyzed silica blanks are consistently below 20 ppm.

2.1.3.2. Pulp duplicates

To assess precision of the results, four pulp duplicates were split from their parent sample after pulverization (Appendix 1, Duplicates-precision). The pulp duplicates represent the homogeneity of the pulp after pulverization, as well as analytical reproducibility (precision). Analytical precision is assessed by performance of the pulp duplicates relative to their parent samples. Relative analytical precision is estimated by the average coefficient of variation, CV_{AVR} (%) of four data pairs (parent-duplicate) (e.g., Van der Vlugt et al., 2022).

$$CV_{AVR}\ (\%) = 100\sqrt{\frac{2}{N}\sum_{i=1}^{N}\left(\frac{(a_i-b_i)^2}{(a_i+b_i)^2}\right)} \qquad \text{Equation 1}$$

where a_i and b_i are the analytical results for the i^{th} pair of duplicate samples, and N is the number of the data pairs (Abzalov, 2008). In cases where analytes were below the detection range for the given method, the values are replaced with ½ LoD (e.g., <5 ppm was replaced with 2.5 ppm) for the calculation of CV_{AVR}. We consider that CV_{AVR} values of <20% to indicate generally acceptable precision. Several key analytes, such as Cu, Ni, Pd, Pt, Te, Te, yield >20% CV_{AVR}. This poor replication of duplicates may be a result of heterogeneity of the pulp, poor analytical precision, or a combination of the two factors.

2.1.3.3. Standards

Two standards were included in the sample stream as pulps (Appendix 1, Standards-accuracy). The results from these reference materials can be used to assess analytical accuracy, which is the analytical result relative to their recommended or certified values and standard deviation (or 95% confidence interval). Standards included Canadian Certified Reference Materials Project CANMET TDB-1 (n=1) and WPR-1 (n=1).

For replicate analyses of standards, accurate or unbiased analytical results for each analyte satisfy the following condition:

$$\frac{|m-\mu|}{2\sqrt{\sigma_L^{2}+\frac{{S_w}^{2}}{n}}}\leq 1 \qquad \text{Equation 2}$$

where m is the average of replicate analyses (or the result if n=1), μ is the recommended or certified reference mean (i.e., expected value/EV), σ_L is the interlaboratory certified standard deviation, n is the number of analyses (i.e., n=1 or 2), and $S_w = CV_{AVR} * m$ (representing analytical precision) (e.g., Van der Vlugt et al., 2022). In cases where analytes were below the detection range for the given method, the values are replaced with ½ LoD (e.g., <5 ppm was replaced with 2.5 ppm) for the calculation. The analytical results for TDB-1 are accurate for all of the elements that have concentration and standard deviation data in the standard. The analytical results for WPR-1 are accurate for all elements, except for V, Cr, Sn, which have values slightly higher than 1. The relatively poor precision (i.e., large CV_{AVR} values), represented by S_w in Equation 2, has the effect of increasing the tolerance for accuracy.

2.2. Scanning electron microscopy-mineral liberation analysis (SEM-MLA)

Polished thin sections were examined using a scanning electron microscope (SEM) and derived backscatter electron (BSE) images. Quantitative mineral abundance maps were determined by mineral liberation analysis (MLA). The SEM work was undertaken at the CREAIT Microanalysis Facility (MAF), Memorial University using a FEI MLA 650 field emission gun SEM equipped with two Brucker silicon drift EDS detectors. The backscatter electron detector was operated at an accelerating voltage of 25 kV. Mineral maps were determined using an accelerating voltage of 25 kV, current of 10 nA, and an electron beam spot size of 5.85. Thin sections were measured in GXMAP (grain-based X-ray mapping) mode where X-ray analyses were triggered for a BSE range of 40 to 255. Each X-ray measurement was acquired for 12 ms on a 1.5 by 1.5 mm frame, with a resolution of 500 by 500 pixels per frame and an imaging scan speed of 16 µsec. Data reduction was performed on the MLA Data View (FEI) software version 3.1.4.683.

Acknowledgments

We thank Steve Regoci, Peter Lightfoot, and Jeremy Hanson of Garibaldi Resources Corp. for supporting this project. They graciously provided access to their geochemical database and drill core repository and played a critical role in facilitating field sampling at Nickel mountain.

References cited

Abzalov, M., 2008. Quality control of assay data: A review of procedures for measuring and monitoring precision and accuracy. Exploration and Mining Geology, 17, 131-144. https://doi.org/10.2113/gsemg.17.3-4.131

ALS, 2024. Geochemistry schedule of services and fees CAD 2024. Last accessed November 28, 2024. https://www.alsglobal.com/en/geochemistry/geochemistry-feeschedules

Brzozowski, M.J., and Zaborniak, K., 2024. Sulphide mineralization at the E&L magmatic Ni-Cu-PGE deposit: Textural evidence for contamination, vapour saturation, fluid immiscibility, and metal remobilization. In: Geological Fieldwork 2023. British Columbia Ministry of Energy, Mines and Low Carbon Innovation, British Columbia Geological Survey Paper 2024-01, pp. 65-78.

Ernst, R.E., and Jowitt, S.M., 2013. Large igneous provinces (LIPs) and metallogeny. In: Colpron, M., Bissig, T., Rusk, B.G., and Thompson, J.F.H., (Eds.), Tectonics, Metallogeny, and Discovery: The North American Cordillera and Similar Accretionary Settings. Society of Economic Geologists Special Publication 17, pp. 17-51.

Humphreys, D., 2014. The mining industry and the supply of critical minerals. In: Gunn, G., (Ed.), Critical Metals Handbook, John Wiley and Sons, pp. 20-40.

Jackson-Brown, S., 2017. Origin of Cu-PGE-rich sulphide mineralization in the DJ/DB Zone of the Turnagain Alaskan-type intrusion, British Columbia. Unpublished M.Sc. thesis, The University of British Columbia, Vancouver, Canada, 290 p.

Manor, M.J., Scoates, J.S., Nixon, G.T., and Ames, D.E., 2016. The Giant Mascot Ni-Cu-PGE Deposit, British Columbia: Mineralized conduits in a convergent margin tectonic setting. Economic Geology, 111, 57-87.

Milidragovic, D., Nixon, G.T., Scoates, J.S., Nott, J.A., and Spence, D.W., 2021. Redox-controlled chalcophile element geochemistry of the Polaris Alaskan-type mafic-ultramafic complex, British Columbia, Canada. The Canadian Mineralogist, 59, 1627-1660.

Mudd, G.M., and Jowitt, S.M., 2014. A detailed assessment of global nickel resource trends and endowments. Economic Geology, 109, 1813-1841.

Mudd, G.M., Weng, Z., Jowitt., S.M., Turnbull, I.D., and Graedel, T.E., 2013. Quantifying the recoverable resources of by-product metals: The case of cobalt. Ore Geology Reviews, 55, 87-98.

Mudd, G.M., Jowitt, S.M., and Werner, T.T., 2018. Global platinum group element resources, reserves and mining-A critical assessment. Science of the Total Environment, 622-623, 614-625.

Petavratzi, E., Gunn, G., and Kresse, C., 2019. BGS commodity review: Cobalt. British Geological Survey, 72 p.

Reich, M., and Simon, A.C., 2025. Critical minerals. Annual Review of Earth Planet Sciences, 53, 141-168. https://doi.org/10.1146/annurev-earth-040523-023316

Van der Vlugt, J., Rukhlov, A.S., and van Straaten, B.I., 2022. Lithogeochemical re-analysis of British Columbia Geological Survey archived rock samples from northwestern British Columbia. British Columbia Ministry of Energy, Mines and Low Carbon Innovation, British Columbia Geological Survey GeoFile 2022-14, 15 p.

BRITISH COLUMBIA

Ministry of
Mining and
Critical Minerals

BRITISH COLUMBIA
est. 1895
GEOLOGICAL SURVEY